

PAPER

# The optical Tamm states at the interface between a photonic crystal and a nanocomposite containing core–shell particles

To cite this article: S Ya Vetrov *et al* 2016 *J. Opt.* **18** 065106

View the [article online](#) for updates and enhancements.

## Related content

- [Optical Tamm states at the interface between a photonic crystal and an epsilon-near-zero nanocomposite](#)  
Stepan Ya Vetrov, Rashid G Bikbaev, Natalya V Rudakova *et al.*
- [The optical Tamm states at the interface between a photonic crystal and nanoporous silver](#)  
R G Bikbaev, S Ya Vetrov and I V Timofeev
- [Spectral and polarization properties of a 'cholesteric liquid crystal—phase plate—metal' structure](#)  
S Ya Vetrov, M V Pyatnov and I V Timofeev

## Recent citations

- [Hybrid Tamm and surface plasmon polaritons in resonant photonic structure](#)  
Rashid G. Bikbaev *et al*
- [Transparent conductive oxides for the epsilon-near-zero Tamm plasmon polaritons](#)  
Rashid G. Bikbaev *et al*
- [Broadband Tamm plasmon polariton](#)  
Andrey M. Vyunishchev *et al*



**IOP | ebooks™**

Bringing together innovative digital publishing with leading authors from the global scientific community.

Start exploring the collection—download the first chapter of every title for free.

# The optical Tamm states at the interface between a photonic crystal and a nanocomposite containing core–shell particles

S Ya Vetrov<sup>1,2</sup>, P S Pankin<sup>1</sup> and I V Timofeev<sup>2,3</sup>

<sup>1</sup> Siberian Federal University, Institute of Engineering Physics and Radio Electronics, Krasnoyarsk, 660041 Russia

<sup>2</sup> Kirensky Institute of Physics, Russian Academy of Sciences, Siberian Branch, Krasnoyarsk, 660036 Russia

<sup>3</sup> Siberian Federal University, Laboratory of Nonlinear Optics and Spectroscopy, Krasnoyarsk, 660041 Russia

E-mail: [ppankin@sfu-kras.ru](mailto:ppankin@sfu-kras.ru)

Received 17 March 2016

Accepted for publication 12 April 2016

Published 11 May 2016



CrossMark

## Abstract

We investigate the optical Tamm states (OTSs) localized at the interface between a photonic crystal (PC) and a nanocomposite consisting of spherical nanoparticles with a dielectric core and a metallic shell, which are dispersed in a transparent matrix, and is characterized by the resonance permittivity. Spectra of transmission, reflection, and absorption of normally incident light waves by the investigated structure are calculated. The spectral manifestation of the Tamm states caused by negative values of the real part of the effective permittivity in the visible spectral range is studied. It is demonstrated that, along with the significantly extended band gap of the PC, the transmission spectrum contains an additional stopband caused by nanocomposite absorption near the resonance frequency. It is shown that the OTSs can be implemented in two band gaps of the PCs, each corresponding to a certain plasmon resonance frequency of the nanocomposite. It is established that the characteristics of the Tamm state localized at the edge of the PCs significantly depend on the ratio between the particle core volume and the total particle volume.

Keywords: photonic crystal, nanocomposite, optical Tamm state, shelled nanoparticles, effective permittivity

(Some figures may appear in colour only in the online journal)

## Introduction

In recent years, there has been an increased interest in the special type of localized electromagnetic states excited at the normal incident of light onto a sample, which are called the optical Tamm states (OTSs) [1, 2]. These states are analogous to the Tamm surface states in physics of condensed matter. They can be excited between two different photonic crystals (PCs) with overlapping band gaps [3] or between a PC and a medium with negative permittivity  $\varepsilon$  [4, 5]. The surface electromagnetic

wave at the interface between the PC and a medium with  $\varepsilon < 0$  is a single unit with the surface plasmon, i.e., oscillations of free electrons near the conductor surface. Such a bound mode of the radiation field and the surface plasmon excitation is called the surface plasmon polariton and is widely used in the visible and infrared spectral ranges for surface investigations. In experiments, the OTS can be observed as a narrow peak in the transmission spectrum of a sample [6, 7].

Surface modes and OTSs can be used in sensors and optical switches [8], multichannel filters [9], Faraday- and

Kerr-effect amplifiers [7, 10], organic solar cells [11], and absorbers [12].

PCs with nanostructured metal–dielectric inclusions offer new opportunities for manipulating light [13–18]. In our previous work [5], we demonstrated the possibility of implementation of the OTSs localized at the edges of a one-dimensional (1D) PC bounded by metal–dielectric isotropic nanocomposite (NC) media on its one of both sides. The NC consists of spherical or spheroidal metal nanoparticles dispersed in a transparent matrix and is characterized by the effective permittivity  $\varepsilon(\omega)$ ; the optical characteristics of the initial materials do not exhibit resonance features. The position of a frequency range where the NC behaves like a metal, i.e.,  $\text{Re}(\varepsilon(\omega)) < 0$ , depends on permittivities of the initial materials and nanoparticle concentration and shape, which opens new possibilities for controlling the optical properties of the OTSs by varying the NC parameters.

The aim of this study was to investigate the spectral properties of the OTSs localized at the edges of a 1D PC bounded by a nanocomposite consisting of spherical nanoparticles with a dielectric core and a metallic shell, which are dispersed in a matrix.

### Description of the model

The investigated PC structure is a layered medium bounded by an NC layer (figure 1(a)). The NC layer with a thickness of  $W_d = 150$  nm consists of shelled layered spherical nanoparticles uniformly distributed in a dielectric matrix from transparent optical glass with a permittivity of  $\varepsilon_m = 2.56$ . The alternating layers that form a PC unit cell are silicon dioxide  $\text{SiO}_2$  with a permittivity of  $\varepsilon_b = 2.10$  and zirconium dioxide  $\text{ZrO}_2$  with a permittivity of  $\varepsilon_a = 4.16$ ; the respective layer thicknesses are  $W_a = 74$  nm and  $W_b = 50$  nm. The investigated PC structure is placed in a medium (air) with a permittivity of unity and consists of 16 layers, including the NC layer.

The effective permittivity of the NC is determined from the Maxwell–Garnett formula [18] widely used in studying composite media. Generalization of this formula to the NC with dispersed core–shell spherical particles yields the effective permittivity [19]

$$\varepsilon = \varepsilon_m \left( 1 + \frac{3f\alpha}{1 - f\alpha} \right), \quad (1)$$

where  $f$  is the filling factor, i.e., the volume fraction of nanoparticles in the matrix and  $\alpha$  is the parameter proportional to dipole polarizability of a layered nanoparticle. The Maxwell–Garnett model for the effective medium suggests the quasi-static consideration of an electrostatically isotropic NC layer with the size of nanoparticles and distance between them much smaller than the light wavelength in the effective medium.

For a spherical particle with core permittivity  $\varepsilon_c$  and shell permittivity  $\varepsilon_s$ , which is placed in a medium with permittivity

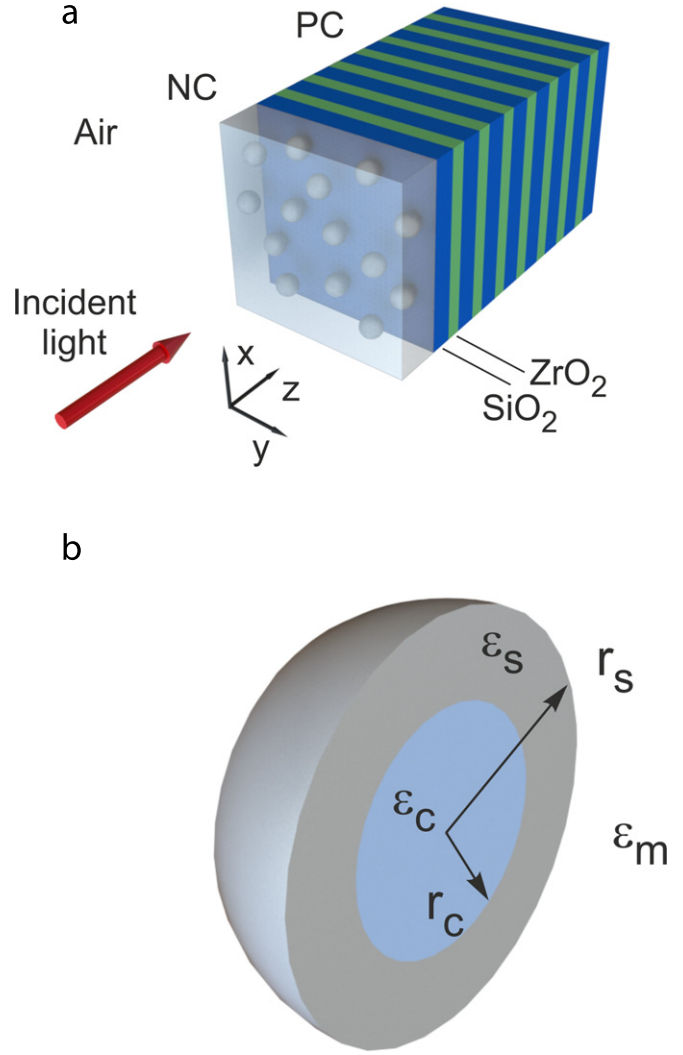


**Figure 1.** (a) Schematic of a 1D PC bounded by a nanocomposite layer and (b) nanoparticle cross section.

$\varepsilon_m$ , parameter  $\alpha$  is determined as [19, 20]:

$$\alpha = \frac{(\varepsilon_s - \varepsilon_m)(\varepsilon_c + 2\varepsilon_s) + \beta(\varepsilon_m + 2\varepsilon_s)(\varepsilon_c - \varepsilon_s)}{(\varepsilon_s + 2\varepsilon_m)(\varepsilon_c + 2\varepsilon_s) + 2\beta(\varepsilon_s - \varepsilon_m)(\varepsilon_c - \varepsilon_s)}, \quad (2)$$

where  $\beta = (r_c/r_s)^3$  is the ratio between the core volume and the total particle volume (figure 1(b)). In the investigated structure, nanoparticles consist of the dielectric core with a permittivity of  $\varepsilon_c = 3$  and the silver shell with permittivity  $\varepsilon_s$  determined from the Drude–Sommerfeld formula

$$\varepsilon_s(\omega) = \varepsilon_0 - \frac{\omega_p^2}{\omega(\omega + i\gamma)}, \quad (3)$$

where  $\varepsilon_0$  is the constant that makes allowance for the contributions of interband transitions of bound electrons;  $\omega_p$  is the plasma frequency;  $\gamma$  is the damping coefficient, i.e., the quantity reciprocal to the electron relaxation time; and  $\omega$  is the frequency of incident light. For silver, we have  $\varepsilon_0 = 5$ ,  $\hbar\omega_p = 9$  eV, and  $\hbar\gamma = 0.02$  eV. At present, there exists the nanoparticle fabrication technology that allows varying the core and shell sizes in wide ranges [21, 22].

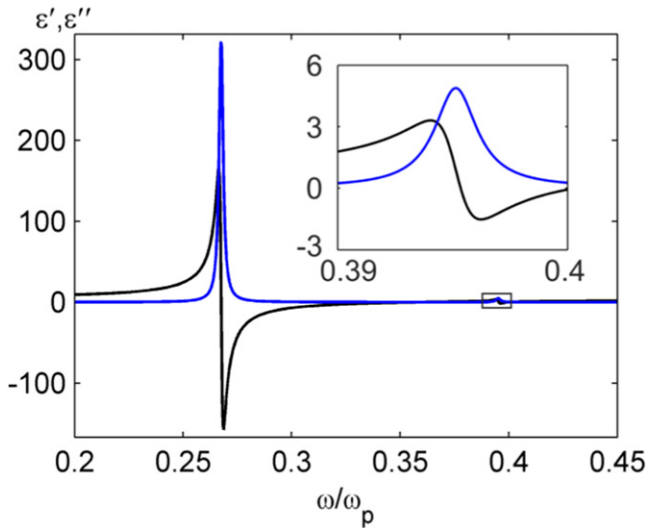


**Figure 2.** Real  $\epsilon'$  (black) and imaginary  $\epsilon''$  (blue) parts of the NC permittivity versus frequency of incident light. Insert: the enlarged framed portion. The parameters are  $f = 0.3$ ,  $\beta = (0.3)^3$ ,  $\epsilon_m = 2.56$ , and  $\epsilon_c = 3$ .

Figure 2 shows the dependence of the effective NC permittivity on the frequency of incident light for the chosen parameters of the NC. One can see two resonance permittivity portions associated with the plasmon resonance of nanoparticles. Surface plasmons arise at the metallic shell/core and metallic shell/matrix interfaces. As the core permittivity

is increased, the high-frequency resonance permittivity portion sharply grows, whereas the long-frequency portion slightly decreases. The opposite situation is observed at the growing permittivity of the matrix. In addition, the both resonances shift toward lower frequencies. As the shell becomes thinner, the coupling between plasmons localized at the shell boundaries becomes stronger and the repulsion of modes is observed; i.e., the high-frequency resonance part of the permittivity moves toward higher frequencies, while the low-frequency part moves toward lower frequencies.

The transmission, reflection, and absorption spectra of the layered structure were calculated using the transfer matrix method [23] for the plane light wave normally incident onto the structure.

### Results and discussion

Figure 3 shows transmission, reflection, and absorption spectra for the PC consisting of 15 layers, which is bounded by the NC layer without nanoparticles and with a nanoparticle fraction of 0.3 in the NC. It can be seen that the spectra qualitatively change upon embedding nanoparticles. At a frequency of about  $0.39\omega_p$  (348 nm), the stopband forms (figure 3(a)), which is associated with absorption of light at the resonance frequency (figure 3(c)) corresponding to the high-frequency resonance portion of the NC permittivity (figure 2). The initial band gap in the transmission spectrum increases due to the high reflection of light (figure 3(b)) at

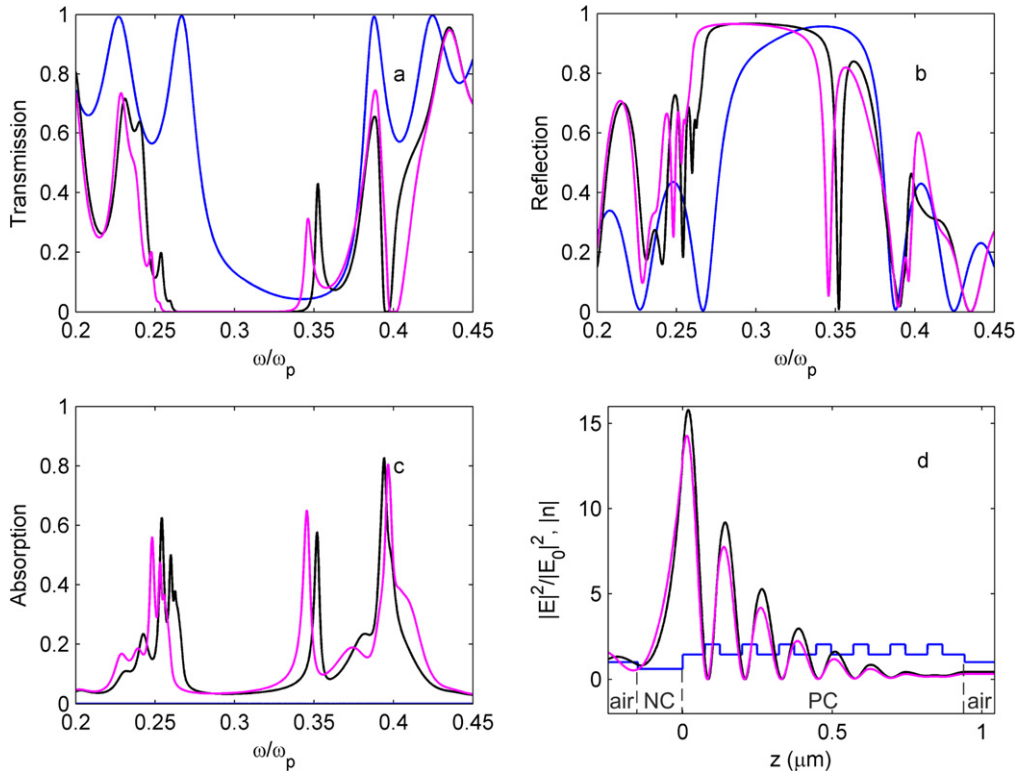


**Figure 3.** (a) Transmittance, (b) reflectance, and (c) absorbance of the PC bounded by the NC layer versus frequency of incident light at filling factors of  $f = 0$  (blue);  $f = 0.3$  and  $\beta = (0.3)^3$  (black); and  $f = 0.3$  and  $\beta = (0.4)^3$  (purple). (d) Spatial distributions of the local field intensity at a frequency of  $0.353\omega_p$  (391 nm),  $f = 0.3$ , and  $\beta = (0.3)^3$  (black) and at a frequency of  $0.346\omega_p$  (398 nm),  $f = 0.3$ , and  $\beta = (0.4)^3$  (purple) and refractive indices of the layers (blue). The parameters are  $W_d = 150$  nm,  $\epsilon_m = 2.56$ , and  $\epsilon_c = 3$ .

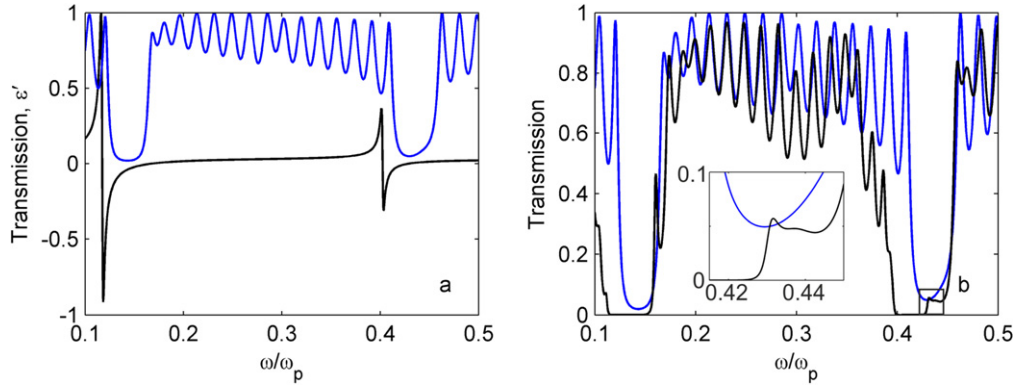


**Figure 4.** Transmittance of the PC bound by the NC layer versus intensity of incident light. The black line in (a) shows the normalized real part of the NC permittivity. The parameters are  $W_d = 150$  nm,  $W_a = 113.5$  nm,  $W_b = 168$  nm,  $\beta = (0.82)^3$ ,  $\epsilon_m = 4$ ,  $\epsilon_c = 10$ ,  $f = 0$  (blue), and  $f = 0.4$  (black).

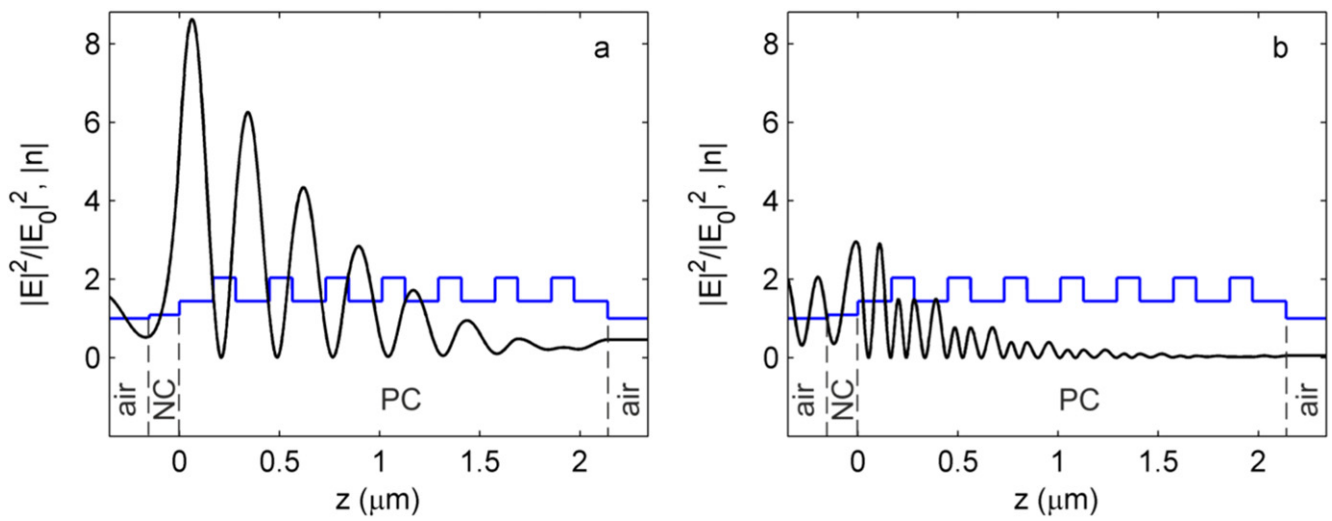


**Figure 5.** Spatial distribution of the local field intensity for the peaks corresponding to the OTSs in figure 4(b) (black) and refractive indices of the layers (blue). The frequencies are (a)  $0.16\omega_p$  (858.8 nm) and (b)  $0.43\omega_p$  (319.2 nm).

these frequencies. The high reflectance is caused by the large negative value of the real part of the NC permittivity (figure 2). In addition, near the high-frequency boundary of the band gap, the transmission peak arises, which is related to the occurrence of the OTS. The light field in the Tamm plasmon polariton is localized in the region comparable with the wavelength. The local field intensity distribution at a frequency of  $0.353\omega_p$  (391 nm) corresponding to the OTS is shown in figure 3(d). The field is localized at the PC/NC interface, since at this frequency the real part of the NC permittivity is negative and the NC behaves like a metal (figure 2); therefore, the field penetrates into it only to the depth equal to the skin-layer thickness. Deeper in the PC, the intensity envelope exponentially decreases due to the Bragg diffraction, since this frequency lies within the PC band gap.

As the ratio between the core and shell radii grows at the invariable initial parameters, the transmission and local field intensity at the OTS frequency decrease. In this case, the reflection weakens, while the absorption is intensified. The transmission peak shifts toward lower frequencies. With an increase in the ratio between the core and shell radii to 0.4,

the transmission at an OTS frequency of  $0.346\omega_p$  (398 nm) decreases by 12%, the absorption increases by 8%, the reflection increases by 4%, and the local intensity decreases by 11% (figure 3).

Selecting the parameters of the structure, we can obtain the coincidence of two regions with the negative real part of the permittivity of the NC with the two corresponding band gaps in the initial transmission spectrum of the PC ( $f = 0$ ) (figure 4(a)). Then, the peak corresponding to the OTS arises near the high-frequency boundaries of both band gaps upon embedding nanoparticles in the NC (figure 4(b)). The local field intensity distribution at frequencies of  $0.16\omega_p$  and  $0.43\omega_p$  (858.8 nm and 319.2 nm, respectively) corresponding to the OTS is shown in figure 5. It can be seen that for both peaks the field is localized at the PC/NC interface.

### Conclusions

The spectral properties of a 1D PC bounded by the nanocomposite layer were investigated. The nanocomposite

consists of spherical nanoparticles with a dielectric core and a silver shell, which are dispersed in transparent optical glass.

It was demonstrated that the transmission spectrum of the investigated structure can simultaneously contain the stop-band related to absorption at the resonance frequency of the nanocomposite permittivity and the transmission peak in the PC band gap corresponding to the OTS caused by the negative real part of the nanocomposite permittivity.

It was shown that at certain parameters of the structure, the spectrum is indicative of the presence of two OTSs in two band gaps of a PC. Such a situation can take place when the portions of the negative real part of the nanocomposite permittivity in the initial transmission spectrum of the PC coincide. It was established that the spectrum of transmission of electromagnetic waves can be effectively manipulated by changing the structural parameters of the PC and nanocomposite matrix and the ratio between the core volume and the total particle volume.

## Acknowledgments

This study was supported by the Ministry of Education and Science of the Russian Federation, state order no. 3.1276.2014/K for the Siberian Federal University in 2016 and Scholarship of the President of the Russian Federation no. SP-227.2016.5.

## References

- [1] Vinogradov A P, Dorofeenko A V, Merzlikin A M and Lisyansky A A 2010 Surface states in photonic crystals *Phys.—Usp.* **53** 243–56
- [2] Kavokin A, Shelykh I and Malpuech G 2005 Optical Tamm states for the fabrication of polariton lasers *Appl. Phys. Lett.* **87** 261105
- [3] Kavokin A V, Shelykh I A and Malpuech G 2005 Lossless interface modes at the boundary between two periodic dielectric structures *Phys. Rev. B* **72** 233102
- [4] Kaliteevski M, Iorsh I, Brand S, Abram R A, Chamberlain J M, Kavokin A V and Shelykh I A 2007 Tamm plasmon-polaritons: possible electromagnetic states at the interface of a metal and a dielectric bragg mirror *Phys. Rev. B* **76** 165415
- [5] Vetrov S Y, Bikbaev R G and Timofeev I V 2013 Optical Tamm states at the interface between a photonic crystal and a nanocomposite with resonance dispersion *J. Exp. Theor. Phys.* **117** 988–98
- [6] Sasin M E, Seisyan R P, Kaliteevski M A, Brand S, Abram R A, Chamberlain J M, Egorov A Y, Vasil'ev A P, Mikhrin V S and Kavokin A V 2008 Tamm plasmon polaritons: slow and spatially compact light *Appl. Phys. Lett.* **92** 251112
- [7] Goto T, Dorofeenko A V, Merzlikin A M, Baryshev A V, Vinogradov A P, Inoue M, Lisyansky A A and Granovsky A B 2008 Optical Tamm states in one-dimensional magnetophotonic structures *Phys. Rev. Lett.* **101** 113902
- [8] Zhang W L and Yu S F 2010 Bistable switching using an optical Tamm cavity with a kerr medium *Opt. Commun.* **283** 2622–6
- [9] Zhou H, Yang G, Wang K, Long H and Lu P 2010 Multiple optical Tamm states at a metal–dielectric mirror interface *Opt. Lett.* **35** 4112–4
- [10] Vinogradov A P, Dorofeenko A V, Erokhin S G, Inoue M, Lisyansky A A, Merzlikin A M and Granovsky A B 2006 Surface state peculiarities in one-dimensional photonic crystal interfaces *Phys. Rev. B* **74** 045128
- [11] Zhang X-L, Song J-F, Li X-B, Feng J and Sun H-B 2012 Optical Tamm states enhanced broad-band absorption of organic solar cells *Appl. Phys. Lett.* **101** 243901
- [12] Gong Y, Liu X, Lu H, Wang L and Wang G 2011 Perfect absorber supported by optical Tamm states in plasmonic waveguide *Opt. Exp.* **19** 18393–8
- [13] Tikhodeev S G and Gippius N A 2009 The scattering matrix and optical properties of metamaterials *Phys.—Usp.* **179** 1027–30
- [14] D'yachenko P N and Miklyaev Y V 2007 Dimensional photonic crystals based on nanocomposite: metal nanoparticles–dielectric *Comput. Opt.* **31** 31–4
- [15] Vetrov S Y, Avdeeva A Y and Timofeev I V 2011 Spectral properties of a one-dimensional photonic crystal with a resonant defect nanocomposite layer *J. Exp. Theor. Phys.* **113** 755–61
- [16] Vetrov S Y, Pankin P S and Timofeev I V 2014 Peculiarities of spectral properties of a one-dimensional photonic crystal with an anisotropic defect layer of the nanocomposite with resonant dispersion *Quantum Electron.* **44** 881–4
- [17] Moiseev S G, Ostatochnikov V A and Sementsov D I 2012 Defect mode suppression in a photonic crystal structure with a resonance nanocomposite layer *Quantum Electron.* **42** 557–60
- [18] Maxwell G J C 1904 Colours in metal glasses and in metallic films *Phil. Trans. R. Soc.* **203** 385–420
- [19] Sihvola A 2008 *Electromagnetic Mixing Formulas and Applications* (London: Institution of Engineering and Technology)
- [20] Klimov V 2014 *Nanoplasmonics* (Boca Raton, FL: CRC Press)
- [21] Oldenburg S J, Averitt R D, Westcott S L and Halas N J 1998 Nanoengineering of optical resonances *Chem. Phys. Lett.* **288** 243–7
- [22] Wong H, Wu Y, Lassiter B, Nehl C L, Hafner J H, Nordlander P and Halas N J 2006 Symmetry breaking in individual plasmonic nanoparticles *Proc. Natl Acad. Sci.* **103** 10856–60
- [23] Yeh P 1979 Electromagnetic propagation in birefringent layered media *J. Opt. Soc. Am.* **69** 742–56